

Estimation of azimuthally varying attenuation from wide-azimuth P-wave data

Ivan Vasconcelos* and Edward Jenner†, *Center for Wave Phenomena, Department of Geophysics, Colorado School of Mines; †GX Technology - Axis Imaging Division

Summary

Observing the azimuthally varying character of seismic attenuation in data that show azimuthal velocity anisotropy could contribute not only to the interpretation of the symmetry systems of the subsurface, but also to the characterization of its physical parameters. In this paper, we estimate of azimuthal variations of the effective quality factor (Q) from field surface seismic data.

By assuming that Q is frequency independent, and the medium at each particular azimuth the medium is laterally homogeneous, we use the spectral ratio method and a regularized linear inversion scheme to estimate the quality factor in azimuth-sectored data. The regularization parameters are chosen by a χ^2 criterion that is based on estimates of the variance in the data. Tests on synthetic data show that this regularized inversion provides robust estimates of Q for signal-to-noise ratios lower than those observed in the data.

Application of this methodology to P-wave data from the East Decatur Field in Texas yields non-negligible azimuthal variations in Q . The azimuthal signature of attenuation appears to be consistent with the effective NMO ellipses from the same interface. However, data residuals show non-random structures that suggest a strong systematic component to the noise. We provide a brief analysis of scattering-related absorption and of frequency imprints of source-receiver arrays as possible sources of systematic noise.

Introduction

An important dynamic effect for wave propagation in elastic media is attenuation. In media containing aligned cracks on scales smaller than the dominant seismic wavelength there should be azimuthally variable signatures of attenuation. Experiments conducted in anisotropic physical models (Arts and Rasolofosaon, 1992) showed that not only attenuation has a directional dependence but also the magnitude of the anisotropy can be more significant than that of velocity. Clark et al. (2001) estimated azimuthal variations of attenuation from four sail-line profiles extracted from a 3D marine dataset acquired offshore West Africa. Their interpretation of the principal orientation of the azimuthally variable attenuation is consistent with fracture orientations inferred from azimuthally variable AVO.

The main goal of this paper is to devise and implement a methodology that allows for azimuthally varying estimates of the quality factor (Q). By assuming our model to be horizontally layered, laterally homogeneous and that Q only varies with azimuth we impose that any two trace

pairs in a certain azimuth should yield the same estimate of Q . In practice we enforce the roughness penalty by means of Tikhonov regularization. Since the reliability of our estimates is an important issue, error estimation is done by linear error propagation (van Wijk et al., 2002). In order to obtain estimates of the variance in the data that are independent of model parameters, we use a non-parametric fitting approach (van Wijk et al., 2002).

Estimating Q

The vast majority of existing methods for Q inversion assume 2D media. In this paper, we assume that any vertical plane represents a section of horizontally layered, laterally homogeneous and isotropic medium. Such assumption allows us to use all data within a given narrow azimuth sector to obtain an estimate of the quality factor at that azimuth.

The quality factor Q can be directly estimated from the slope of the ratio of the spectra (in logarithmic scale) for any two traces, if the difference in traveltime between the traces is known. This is the so-called spectral ratio (SR) method for inverting for Q (Mateeva, 2003). In the simple line regression framework of the spectral ratio method, the absorption-related effects are contained in the slope term (frequency dependent), whereas all frequency-independent (AVO, geometrical spreading) effects are contained in the intercept term.

Since the spectral ratio method assumes a homogeneous model, estimates of the quality factor for different trace pairs for a gather with a fixed azimuthal orientation should be the same. The methodology presented here seeks to take advantage of this “redundancy” by introducing a regularization operator. If there are N possible trace combinations in our azimuth gather, we can take the i^{th} trace pair and write our inverse problem based on the SR method in the form of the following linear system:

$$\mathbf{A}_i \mathbf{m}_i = \mathbf{d}_i, \quad (1)$$

where \mathbf{A}_i is the forward operator, containing the frequency samples and the traveltime difference between the two traces in the i^{th} trace pair. The vector \mathbf{m}_i contains the intercept and slope (proportional to $1/Q$) model parameters from the SR method. \mathbf{d}_i is the data vector of spectral ratio samples.

Our model objective function to be minimized in the inversion is designed in the following manner:

$$f(\mathbf{m}_i, \mathbf{s}) = \sum_{i=1}^N \|\mathbf{A}_i \mathbf{m}_i - \mathbf{d}_i\|^2 + \lambda^2 \|\mathbf{R}\mathbf{s}\|^2; \quad (2)$$

\mathbf{s} is a $N \times 1$ matrix whose elements are the slope model parameters from all \mathbf{m}_i ($1/Q$), \mathbf{R} is a regularization matrix and λ is its regularization weighting parameter. This particular choice of \mathbf{s} assures that we regularize our inverse problem only with respect to the slope terms in the SR method, without imposing any assumptions on the frequency-independent intercept term. The first term in equation (2) seeks to minimize the total misfit between the data (the spectral ratio) measured for each trace combination and data predicted by its corresponding \mathbf{m}_i . Acknowledging the existence of non-negligible variance in our data, the second term in equation (2) penalizes the norm of \mathbf{R} times the model. In our case, \mathbf{R} is the sum of the first and second derivative operators.

It is crucial to provide meaningful model variances, such that the final results can be properly interpreted. The variance in the model parameters can be directly estimated from the regularized pseudo-inverse operator and the data covariance matrix (van Wijk et al., 2002). To estimate the variance in the data ($\sigma_{d,i}$) we follow the non-parametric fitting approach described in van Wijk et al. (2002). In our particular application we expect the data to have a linear dependence on frequency, hence we choose the regularization matrix in the nonparametric inverse to be a second derivative operator.

Synthetic data example

The synthetic data were modeled for a single homogeneous, isotropic, attenuative layer with P-wave velocity $V = 2.0\text{km/s}$, $Q = 250$, a reflector depth of 1km and a Ricker source wavelet. The power spectra were contaminated with Gaussian random noise. Noise variances in the synthetic spectra were chosen to be at least two orders of magnitude larger than that from field data traces for time intervals before the first arrival. Before estimating the regularized inverse solution, we estimate $\sigma_{d,i}$ (the variance in the data). For the data with higher offset differences between the two traces the corresponding σ_d is smallest. This happens because all power spectra had their samples randomly distorted with the same variance and the ratios that correspond to spectra with a higher attenuation difference will show smaller variance. If the noise is limited to random fluctuations in the power spectra, traces with larger offset differences will give more stable estimates of Q .

We can also use the estimate for the data variance to get a misfit threshold for the model estimation, by setting the value of χ^2 to some chosen confidence level (e.g. $\chi^2 = 1$, the 68% confidence level). Figure 1a shows that the regularized inverse solution is closer to the true model than the standard generalized least squares (GLS) solution. Figure 1b shows the fit of the regularized and GLS solutions, and for most trace pairs it is hard to visually distinguish the regularized from the non-regularized fit. This difference is small because the traveltime difference between traces is small, which translates into small differences in attenuation magnitudes. However, the differences between the regularized and non-regularized solutions for the same data are quite noticeable. In other

words, estimates of Q from spectral ratios are very sensitive to noise, this is precisely the reason why it is necessary to introduce a regularization operator.

East Decatur field data

Our field data study was conducted on prestack 3-D wide-azimuth P-wave data acquired over the East Decatur field, located in North Texas. The formation of interest, The Barnett shale, is one of the largest producing gas reservoirs in the United States, and it has been reported that its best production rates come from wells drilled in areas where natural fractures were present. Apart from the structural simplicity, this particular dataset was chosen for pronounced lateral variations of the P-wave azimuthal anisotropy. Figure 2a,b shows NMO ellipse parameters for the reflection at the bottom of the Barnett formation. For this field, azimuthal anisotropy is mainly attributed to fractures in the Barnett shale beds since the interval NMO ellipse orientations coincide with fracture orientations from well observations and geologic data.

Here, we show the azimuthal attenuation analysis for two 9X9 superbins, hereafter referred to as CMP1 (Fig. 2) and CMP2, respectively. Traces were then sorted into 5° azimuth bins and the inversion for each bin was conducted for the horizon interpreted as the reflection from the bottom of the Barnett formation. The real data spectra are smoother than that of synthetic data (not shown) because random noise levels for the field data are likely smaller than those in synthetic tests. However, although there is little random noise in the spectra, we observe pronounced, repeatable, nonlinear structures in the spectral ratios (not shown).

To find the value of Q for a given azimuth (Figure 2c), we chose to take the median of the regularized Q measurements for each trace pairs to minimize the contribution of outliers. It is clear from Figure 2c that if our assumptions and estimates of the variance in the data are accurate, there is a non-negligible azimuthal signature of attenuation. The direction of maximum attenuation (lowest Q) is close to the semi-minor axis of the NMO ellipse, approximately oriented East-West (Figure 2b). If the fractures in the shale are gas-filled, a possible physical interpretation is that waves traveling perpendicular to the most prominent set of fractures should have smaller velocities and experience higher attenuation. It is also interesting to observe that the magnitude of azimuthal attenuation anisotropy is much larger than that of azimuthal NMO velocity anisotropy.

For our particular dataset, it is also important to find out if multiple scattering due to thin layering could add a nonlinear component to the spectral ratios, and if this component has a structure that correlates to that observed in the data. Using velocities (compressional and shear-wave) and densities from well logs, we generated a synthetic seismogram for East Decatur with the full elastic wave-field with all multiples and no intrinsic absorption. Figure 3a shows that there is a clear offset-dependent non-

linear frequency imprint of scattering-induced attenuation in the spectral ratios. The data structure in Figure 3a is somewhat different from that observed in field data (not shown), as field structures not only vary with offset, but also differ from one azimuth bin to another. Even though layering-induced absorption causes nonlinear behavior in the spectral ratios, its influence should be azimuthally independent, as long as the medium is laterally homogeneous.

The use of source and receiver arrays in acquisition creates frequency signatures that may distort the spectral ratios. We computed these frequency signatures from the transfer functions of the source-receiver arrays for East Decatur data (Figure 3b,c). Because the spacing between the sources is considerably bigger than that between receivers in their respective arrays, the source array produces a more substantial distortion in the power spectra. Also, there is an azimuthal dependence of the source-receiver transfer function because the sources are set in a line with a fixed orientation for any source-receiver azimuth (Figure 3b,c). The maximum contribution of the source array occurs at the source-receiver azimuth that coincides with the source array orientation (at an azimuth of $45^\circ N$), and the minimum corresponds to the orthogonal direction.

Discussion and Conclusions

With the objective of estimating the azimuthally varying attenuation, we proposed a methodology that assumes that at each azimuth the medium can be considered, as horizontally layered and laterally homogeneous. In the regularization we use equally weighted first and second derivatives operators to impose smoothness on the estimates of Q within each azimuth bin. This methodology is also designed to provide reliable error estimates. The variances in the model parameters are computed from the regularized pseudo-inverse operator and from the data variances obtained with a nonparametric fitting technique. The estimates for data variance also provide the basis for choosing the regularization weighting parameter.

Noisy synthetic data were generated by distorting power spectra with uncorrelated Gaussian noise. For this type of noise, estimates of Q from traces with larger traveltimes differences tend to be more stable because the data variances are smaller. This synthetic test shows that even for signal-to-noise ratios smaller than those typically observed in real data, the regularized inverse estimator predicts the true model within the 90% confidence interval.

In the East Decatur dataset, we applied our inversion methodology to two 9×9 CMP-sorted superbins that lie within one of the areas of strongest azimuthal velocity anisotropy. In this context, our results for the inversion for Q in 5° azimuth sectors from both superbins show a similar azimuthally variable signature. The direction of the maximum attenuation is approximately East-West, which coincides with the average orientation of the semi-minor axis of the P-wave NMO ellipse. Taking gas-

filled fractures with a single predominant orientation as a model for the Barnett shale, maximum attenuation occurs in the direction perpendicular to the fracture strike. An important observation is that the magnitude of the azimuthal variations of attenuation is much larger than that of NMO velocities. This observation suggests that attenuation measurements are much more sensitive to the anisotropy induced by the presence of fluid-filled cracks.

We considered two possible causes for systematic noise in the spectral ratios: absorption effects due to thin layering and frequency distortions caused by stacking the response of source and receiver arrays. For a horizontally layered, laterally homogeneous medium, attenuation effects due to multiple scattering introduce an offset-dependent bias in Q but these are independent of azimuth. The source and receiver arrays introduce an apparent azimuthally variable attenuation effect due only to the source and receiver array geometry, where attenuation is strongest at the $45^\circ N$ direction and weakest at $135^\circ N$.

The methodology presented here could be applied to trace clusters with different offset ranges to obtain an estimate of the dependence of attenuation with polar angle. With closed form expressions for anisotropic attenuation in terms of anisotropic parameters as in Zhu and Tsvankin (2005), the methodology described here could be applied to characterize anisotropic attenuation. Furthermore, our inversion procedure can be applied to other types of datasets with redundant wave-field information (e.g. walkaway vertical seismic profiles, tomographic experiments), and to time lapse studies.

Acknowledgements

We are grateful to Roel Snieder (CWP) for his help on the issue of array transfer functions. Also, we thank GX Technology (AXIS Imag. Div.) and Devon Energy for giving permission to publish these results.

References

- Arts, R. J., and Rasolofosaon, P. N. J., 1992, Approximation of velocity and attenuation in general anisotropic rocks: 62nd Ann. Intl. Mtg. Soc. Expl. Geophys., Expanded Abstracts, 640-643.
- Clark, R. A., Carter, A. J., Nevill, P. C., and Benson, P. M., 2001, Attenuation measurements from surface seismic - azimuthal variation and time lapse case studies: 63rd EAGE Conference and Technical Exhibition, Expanded Abstracts, L-28.
- Mateeva, A., 2003, Thin horizontal layering as a stratigraphic filter in absorption estimation and seismic deconvolution: Ph.D. thesis, Colorado School of Mines.
- van Wijk, K., Scales, J. A., Navidi, W., and Tenorio, L., 2002, On estimating errors in inverse calculations: Geophysical Journal Intl., **149**, 624-632.
- Zhu, Y., and Tsvankin, I., 2005b, Attenuation anisotropy and P-wave propagation in attenuative orthorhombic media: CWP Project Review.

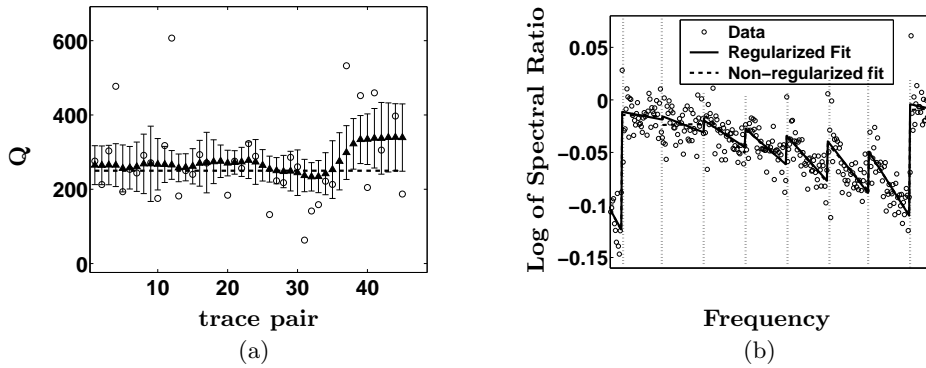


Fig. 1: Inversion results for the synthetic data. The power spectra that generated data for (b) are distorted with twice the variance as the spectra from field data. In (b), data between each pair of vertical dotted lines pertains to a different trace pair. (a) shows the Q estimates from the Tikhonov generalized least squares solution (TGLS, 2^{nd} order stands for the use of a first and second derivative operators in R, Appendix A) and the standard generalized least squares. The error bars represent the variance in the model parameters. (b) contains the models fitted to the data, where the regularized fits are related to the TGLS solutions and the non-regularized fits pertain to the GLS solutions.

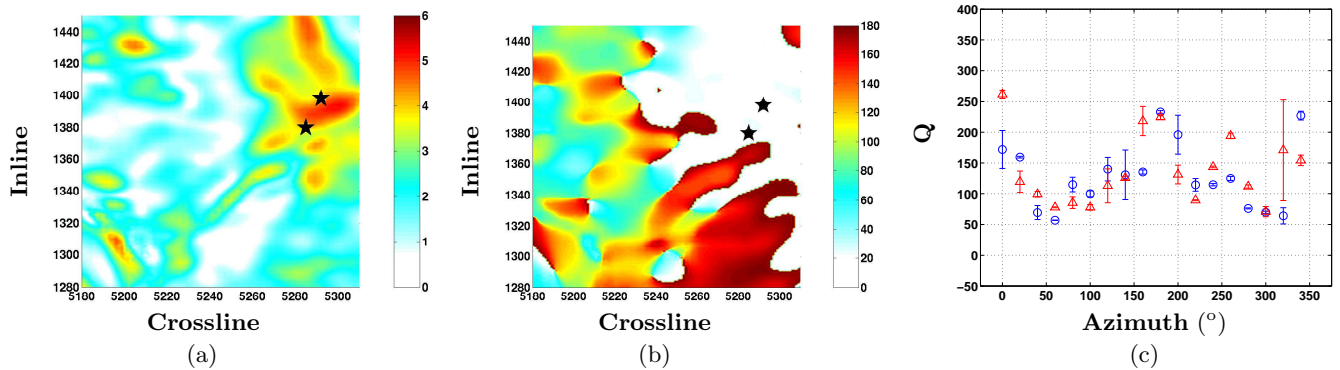


Fig. 2: Azimuthal anisotropy attributes estimated for the reflection from the bottom of the Barnett formation in the East Decatur field. (a) The magnitude of azimuthal anisotropy (NMO ellipse eccentricities) in percent. (b) The orientation of the semi-major axis of the NMO ellipses with respect to North. The two CMPs analyzed (CMP1 and CMP2, indicated by the black stars) lie within the area of stronger azimuthal anisotropy in the upper right-hand corner of the area, respectively with coordinates (*Inline* 1380, *Crossline* 5285) and (*Inline* 1392, *Crossline* 5292). Increasing *Crossline* coordinates point to the North. (d) Azimuthally varying attenuation estimates. The results from CMP1 are marked by the blue circles, and from from CMP2 by red triangles. The error bars in (b) are computed as the average standard deviation of the model variances for all trace pairs within a sector.

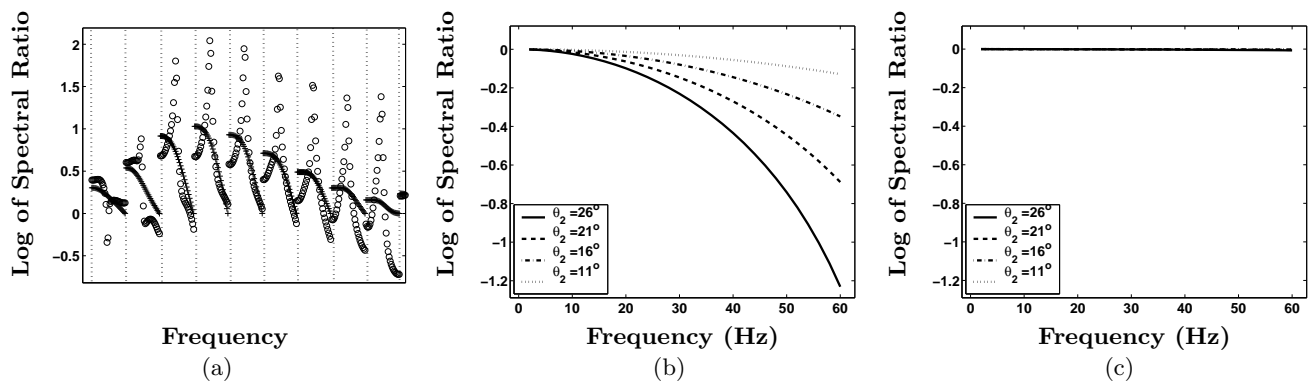


Fig. 3: Influence of systematic noise components in spectral ratio data. (a) Data vectors \mathbf{d}_i (circles) and their smoothed versions (crosses), used to predict the variance in the data. The data in (a) are computed for the same bandwidth as the spectral ratios for the field data: 25-50 Hz. Again, the vertical dotted lines separate data from different trace pairs. (b) and (c) are the spectral ratio signatures due to the source and receiver arrays with azimuths $45^\circ N$ and $135^\circ N$, respectively. Each curve on (b) and (c) ratio plots is computed between one of the signals with the from the legend and a signal with the 5° emergence angle. These emergence angles are directly related to offsets.